

# Short Papers

## Dielectric Resonator Filters with Wide Stopbands

R. V. Snyder

**Abstract**—Use of dielectric resonators in filter networks enables construction of small, low-loss, stable filters. However, such resonators present a modal spectrum with undesired, or spurious, resonances in close proximity to the desired one. Through the use of evanescent mode band-pass irises tuned to the filter center frequency, the resonator spurious modes are suppressed, resulting in N-section filters with stopbands clean to at least (N-1) times the individual iris stopband levels. The tuned irises contribute a small amount of insertion loss but also further reduce the size of the composite filter as compared to a conventional design. The problem of achieving a wide stopband is thus reduced to the more or less well-known problems of realizing the resonating capacitance required in an evanescent bandpass filter plus the computation of the junction susceptance occurring at the interface between a larger evanescent section (the resonator enclosure) and the smaller iris opening. The technique to be described results in high-Q resonator filters with stopbands clean to at least  $-55$  dBc, out to at least 1.7 times the filter center frequency.

### INTRODUCTION

High-Q dielectric resonators have been used in filter structures at least since 1968 [1]. A variety of configurations have been developed, including the original single-mode designs, dual mode, etc. Inter-resonator coupling has been accomplished by separation within a below-cutoff section of waveguide, inductive windows and other irises, coupling screws, puck orientation, notches in walls, and probably a myriad of other combinations [2]–[5].

The high-Q resonators allow for the design of narrow band, low loss filters, with excellent ultimate rejection characteristics. However, the mode chart for all such resonators is crowded: undesired modes are in close proximity both to the desired dominant mode and to each other. Compounding the problem is the fact that the resonators are enclosed in, and are coupled by, below cut-off (evanescent) sections or structures which allow propagation of the higher frequency (“spurious”), modes of resonance more readily than the desired resonant frequency.

One solution to this dilemma is to tailor the coupling structure such that it rejects the spurious modes while accepting a known amount of the desired mode. Recognition that evanescent propagation is essential to the coupling structure of any selective filter immediately suggests treating the coupling structure as a separate evanescent-mode bandpass filter, with a transfer function equal to the desired conventional inter-resonator coupling coefficient. Such coupling coefficients are readily calculated from prototype element values [6], [7]. These calculations are independent of the nature of the high-Q resonator. Thus, the same approach suggested herein should be applicable to interstage couplings within high-Q cavity filters, which also display the same sort of crowded mode chart. The high-Q properties of the dielectric (or cavity) resonators can

be utilized, without external filtering, to achieve fixed or tunable narrow band filters with low passband loss and wide, spurious-free stopbands.

The new principle: Resonated, evanescent-mode bandpass irises are used to filter out the undesired modes, with only a small additional insertion loss as a price.

The problem of achieving a wide stopband is thus reduced to realization of the capacitance needed to resonate the shunt elements of the inductive-Tee or Pi equivalents to a length of evanescent waveguide (the iris) [8]–[10], plus the computation of the susceptive equivalent circuit associated with the junction of a larger evanescent section (the resonator enclosure) and the smaller iris opening [11].

### BASIC STRUCTURE

The technique is illustrated by the example in Fig. 1. The structure consists of high Q dielectric resonators separated by resonated (“tuned”) sections of evanescent waveguide. The dielectric “pucks” are supported on low dielectric constant supports. For low power applications, supports can be made out of Rexolite, low dielectric constant foam, or similar materials. For higher power situations, thermally conductive, low dielectric constant ceramics are available. The pucks are selected to free-space resonate in the dominant  $TE_{016}$  mode, at a frequency somewhat below the desired ultimate operating center frequency. This is due to the “frequency pushing” effect of the enclosure metal walls on the resonator magnetic field. The closer the walls, the more compensation is required. The enclosure dimensions must be such as to ensure that the field is essentially confined to the puck region, i.e. the enclosure must be below cutoff in every dimension, to the operating mode of the puck. At the junction between the puck enclosure and the iris, a susceptive discontinuity is generated due to reflections [11]. A combination of this discontinuity, iris transverse dimensions (cutoff frequency) and axial dimensions (attenuation for the given cutoff), and resonating capacitance then can be used to achieve a wide range of interstage coupling coefficients at the puck resonant frequency, with a large reduction in coupling coefficient occurring at frequencies away from the desired one.

The resonated iris “selects” primarily the dominant enclosure mode at the *desired* center frequency and passband (due to iris location, cross-section and orientation) and “rejects” any modes at *higher* frequencies (due to the resonating capacitance).

The resulting hybrid circuit which can be used for analysis is shown in Fig. 2. The puck resonant frequency in the presence of the walls can be closely approximated by

$$\beta \tan(\beta L/2) = \alpha \quad (1a)$$

where

$$\beta = 2\pi\sqrt{(\epsilon_r/\lambda_o^2) - (.68/D^2)} \quad (1b)$$

$$\alpha = 2\pi\sqrt{(.68/D^2) - (1./\lambda_o^2)} \quad (1c)$$

$D$  = Puck diameter (inches)

$L$  = Puck length (inches)

$f_r = 11.803/\lambda_o$  (GHz).

Manuscript received March 19, 1992; revised May 4, 1992.  
The author is with RS Microwave Company, Inc., 22 Park Place, Butler, NJ 07405-0273.

IEEE Log Number 9202903.

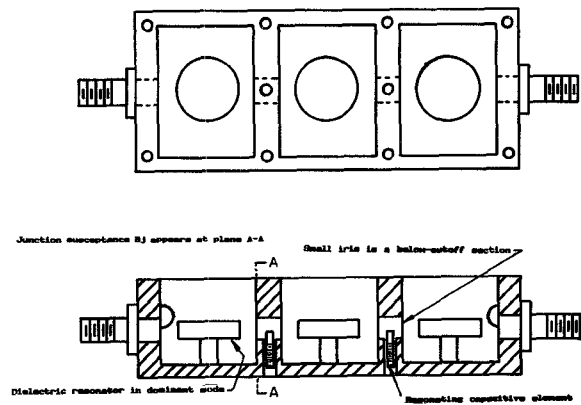


Fig. 1. Basic structure of the new filter.

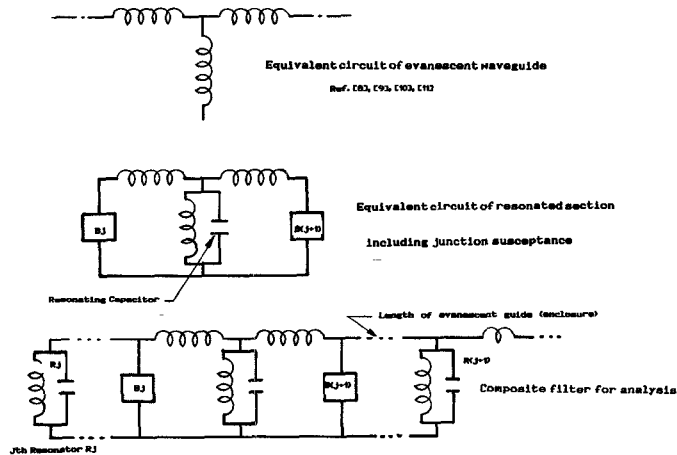


Fig. 2. Equivalent circuits of composite filter.

Equations (1a) and (1b) are modifications of the equations in [1], modified to compensate for the metal wall proximity, and can be iteratively solved for the resonant frequency in the  $TE_{016}$  mode.

Propagation of energy within the enclosure is given by (21) and (45) of [1], repeated below for convenience. It turns out that the evanescent mode bandpass irises do such an excellent job of selecting only one mode that the difference between a mode-matched solution at the iris junction and the assumption of single-mode puck coupling is lost in the tuning of the filter. Thus, the single mode assumption is sufficiently accurate even for the close proximity of enclosure walls and puck which occur in the filter designs under consideration in this paper.

$$F = 0.927D^4L\epsilon_r/\lambda_0^2 \quad (2) \quad (21) \text{ of [1]}$$

$$k = F[\sum \alpha_{mo} e^{-\alpha_{mo}} = +2\sum (\alpha_{mo}^2/\alpha_{mn}) e^{-\alpha_m s}/ab] \quad (3a) \quad (45) \text{ of [1]}$$

multimode coupling

$$k = F\alpha e_{10}^{-\alpha} s/ab \quad (3b) \quad (46) \text{ of [1]}$$

single- $TE_{10}$  mode

Equation (3b) is also used to compute coupling through a non-resonated iris:

$k$  = coupling of puck to puck in the enclosure, without an iris  
(3a) or through a rectangular iris (3b)

$a$  = enclosure width

$b$  = enclosure height

$\alpha_{mn}$  = attenuation in enclosure, in Nepers/meter for  $mn^{\text{th}}$  mode

$s$  = puck-to-puck spacing for the desired coupling coefficient, without any irises.

Because the final iris lengths are much less than the spacing between pucks, it has been found effective to use  $s/2$  as a starting point for the spacing of the puck center to the junction with an iris. Thus, the iris represents a transformation of the magnetic dipole moment of a resonator, from the enclosure-iris interface, through the iris, to the next iris-enclosure interface.

The junction susceptance is given by (7) and (8) of [11] (for the junction of a rectangular enclosure with a rectangularly shaped iris opening).

A quite similar expression can be derived for the junction of a rectangular enclosure with a round, cylindrical iris. However, it is found that the junction susceptance is such a small part of the coupling coefficient for practical, reasonably long irises, that (7) and (8) of [11] can be used by simply replacing the  $a$  and  $b$  dimensions (height and width of the iris) by the diameter of the round iris multiplied by 1.707. Similarly, (3b) can be used by utilizing the same substitution.

To perform the design, coupling through the iris is first modeled without resonating the iris. Under a single mode assumption, the coupling is given by (3b), with  $\alpha_{10}$  computed from the particular iris cross section employed, as a real attenuation constant. If a round cross section is used, "ab" is replaced by  $1.707 d$ , where  $d$  is the iris diameter. However, the single-mode assumption is not valid unless the iris is configured (i.e. oriented, dimensioned and located), to select primarily the dominant mode at  $F_o$ . Fig. 2 illustrates the case in which only one resonating element is used in an iris. The coupling coefficient can clearly be computed from the ladder cascade shown [8]–[10], and can be set equal to the coefficient computed from (3b), at center frequency. As a single-section bandpass filter, the iris will approach a  $-6$  dB/octave slope. The suppression of any higher frequency modes can thus be easily calculated by evaluating the iris attenuation at the particular modal frequency. As stated earlier, the composite mode suppression then becomes the resultant of a cascade of  $N-1$  irises, for an  $N$  pole filter. It is also possible to design more selective irises, by designing the irises as higher-order filters (adding more resonating capacitors spaced in accordance with the design principles for evanescent mode filters as in [8]–[10] and [11]).

No mode matching or optimization is necessary to design these filters. It is only required to do an iterative solution within the cascade shown in Fig. 2, to extract each iris length, after the required coupling coefficient is determined and the desired iris diameter selected. Alternatively, each iris diameter can be extracted, given a selection of iris length and coupling coefficient. It is convenient to perform these iterative solutions using MATHCAD [12], a commercial equation solver. The iris coupling coefficient is then set equal to the coupling coefficient resulting from inclusion of a resonating capacitor, as described above. Equating these coefficients at center frequency necessitates iterative adjustment of iris diameter or length, also using MATHCAD. At lower frequencies, the resonating capacitor may take the form of a re-entrant coaxial section, a lumped capacitor, or similar.

The total design can easily be analyzed using all four terms of the scattering matrix for each element of Fig. 2. However, for the narrow band filters discussed herein, it is not been found necessary to do this, as the tunable irises provide flexibility.

## RESULTS

Measurements on a two resonator, one iris filter with a center frequency of about 5900 MHz indicate about 11 dB suppression of the first spurious mode ( $F_o = 7700$  MHz) when the iris is tuned,

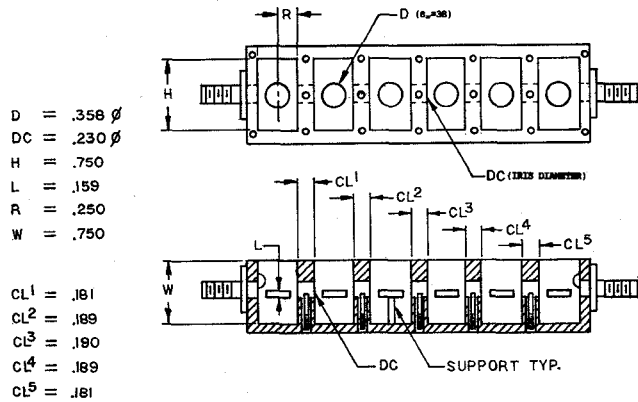
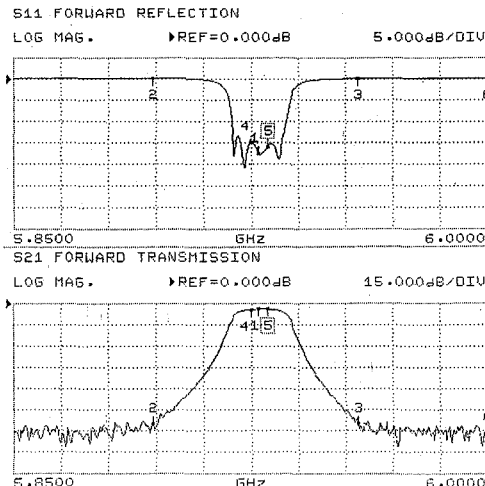
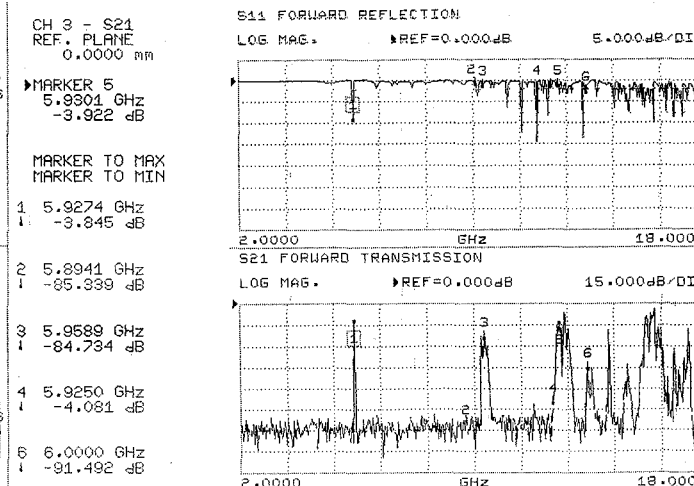


Fig. 3. Six pole filter design example.



(a)

Fig. 4. Responses of 6 pole design example. (a) Passband, 6 pole filter.  
(b) Passband/spurious, 6 pole filter.

(b)

as compared to without iris tuning and about 13 dB, as compared to free space coupling of the two resonators. A 6 resonator, 5 iris unit with  $F_o = 5930$  MHz was constructed. The unit is shown in Fig. 3. The overall response is shown in Fig. 4(a) and (b). The spurious suppression is at least  $-57$  dBc up to 10.3 GHz, relative to the passband loss. The free-space coupled prototype displayed insertion loss which corresponded to an unloaded resonator Q of 6100 at a center frequency of 5900 MHz. The 6 pole, tuned iris unit shown in Fig. 3 displays an unloaded Q value of about 5500, showing approximately a 10% reduction due to both the close proximity of the enclosure walls and the losses in the tuned irises. Similar units have been constructed at center frequencies from about 1 GHz to 15 GHz, with similar results.

### CONCLUSIONS

Resonated evanescent-mode bandpass irises can be combined with high Q cavity resonators to provide the advantages of the high Q resonators with the wide stopbands associated with evanescent mode bandpass filters. The technique should also be applicable to the shunt-coupled resonator (bandstop filter) case, as well. Application of these tuned-irises to cavity filter designs only requires an equivalent circuit and mode chart for the particular cavity resonator to be employed. The design approach does not require optimization, although field-theoretic mode matching methods also are use-

ful for accurate characterization of the enclosure (cavity) interface with the irises and with characterization of the resonating capacitor, particularly at lower frequencies. The new approach should prove useful in a wide range of applications.

### REFERENCES

- [1] S. B. Cohn, "Microwave bandpass filters containing high-Q dielectric resonators," *IEEE Trans. Microwave Theory Tech.*, Apr. 1968.
- [2] J. Plourde and C. Ren, "Dielectric resonators in microwave components," *IEEE Trans. Microwave Theory Tech.*, Aug. 1981.
- [3] J. Fiedziusko *et al.*, "Narrow bandpass dielectric resonator filter with mode suppression pins," U.S. Patent 4 692 723, Sept. 1987.
- [4] K. A. Zaki, C. Chen, and A. Atia, "Canonical and longitudinal dual-mode dielectric resonator filter without iris," *IEEE Trans. Microwave Theory Tech.*, Dec. 1987.
- [5] K. Zaki and S. Chen, "A novel coupling method for dual-mode dielectric resonator and waveguide filters," *IEEE Trans. Microwave Theory Tech.*, Dec. 1990.
- [6] A. Zverev, *Handbook of Filter Synthesis*. New York: Wiley, 1967.
- [7] G. Matthaei, L. Young, and E. Jones, *Microwave Filters, Impedance-Matching Networks, and Coupling Structures*. New York: McGraw-Hill, 1964.
- [8] G. Craven and C. Mok, "The design of evanescent mode waveguide bandpass filters for a prescribed insertion loss characteristic," *IEEE Trans. Microwave Theory Tech.*, Mar. 1971.
- [9] C. Mok, D. Stopp, and G. Craven, "Susceptance-loaded evanescent mode waveguide filters," *Proc. Inst. Elec. Eng.*, Apr. 1972.

- [10] R. Snyder, "New application of evanescent mode waveguide to filter design," *IEEE Trans. Microwave Theory Tech.*, Dec. 1977.
- [11] —, "Broadband waveguide or coaxial filters with wide stopbands, using a stepped-wall evanescent mode approach," *Microwave J.*, Dec. 1983.
- [12] MATHCAD, by MATHSOFT, Cambridge, MA.

## Analysis and Modeling of Coupled Dispersive Interconnection Lines

T. Dhaene, S. Criel, and D. De Zutter

**Abstract**—In this short paper, we present a standard method for the analysis and the simulation of coupled dispersive interconnection structures. A high-frequency circuit model is proposed which is well-suited for CAD applications. A lot of attention is paid to the physical interpretation of the full-wave parameters.

### INTRODUCTION

A large number of publications deal with the calculation of the hybrid-mode characteristics of coupled interconnection structures. The general waveguide structure with  $N$  propagating fundamental modes is completely characterized by  $N(N + 1)$  complex frequency dependent parameters. These parameters can be the  $N^2$  line-mode characteristic impedances  $Z_{ip}$  and the  $N$  modal propagation factors  $\gamma_p$  which follow directly from the full-wave analysis. Quite often, the meaning of the so-called "line-mode characteristic impedance"  $Z_{ip}$  (associated with conductor  $i$  and eigenmode  $p$ ) is misunderstood and there is some confusion between this line-mode characteristic impedance and the circuit-oriented characteristic impedance matrix  $Z_c$ , which relates the circuit voltages and currents. This can lead to incorrect calculations and wrong interpretations.

Until now, the full-wave data are not often used for transient simulation [1]–[2]. In this paper a high-frequency circuit model is presented for the simulation of coupled dispersive interconnection structures. A frequency dependent circuit model is required if the dispersive nature of such a structure has to be taken into account. A simple two-line system, earlier described by Fukuoka *et al.* [3], is used as typical example. Emphasis is on the application and interpretation of the circuit model. The complete theoretical background of the model is presented elsewhere [4]. Based on the correct interpretation of the line-mode impedance and the circuit impedance, a new and to our understanding more correct physical interpretation of the different relevant parameters is given.

### FULL-WAVE CIRCUIT MODEL

Consider a general multiconductor transmission line structure with  $N$  conductors and a reference conductor. For such hybrid interconnection structures, the conductor voltages  $V_c(z)$  and currents

Manuscript received November 19, 1991; revised May 1, 1992. This work was supported by a grant to the first author from the IWONL (Instituut tot Aanmoediging van het Wetenschappelijk Onderzoek in de Landbouw en de Nijverheid) and by a grant to S. Criel from the NFWO (National Fund for Scientific Research of Belgium). D. De Zutter is Senior Research Associate for the NFWO.

The authors are with the Laboratory of Electromagnetism and Acoustics, University of Ghent, Sint-Pietersnieuwstraat 41, 9000 Ghent, Belgium.

IEEE Log Number 9202904.

$I_c(z)$  cannot be calculated in an unambiguous way as line-integrals of the electric and magnetic fields.  $V_c$  is a vector consisting of elements  $V_{ci}(i = 1, \dots, N)$  where  $V_{ci}$  is the circuit voltage associated with conductor  $i$ .  $I_c$  is defined in an analogous way. Only in the quasi-static limit, both circuit parameters, voltage and current, have a unique and clear circuit interpretation.

We use the well-accepted *PI-formulation* [4]–[5] to model the structure under study. This approach is well-suited for microstrips, striplines and related structures. The circuit current  $I_{ci}(z)$  is chosen to be identical to the total longitudinal current flowing along conductor  $i$ . Furthermore, both the circuit model and the real waveguide structure are required to have the same complex modal propagation factors and to propagate the same average complex power. This leads to the generalized frequency dependent telegrapher's equations:

$$-\frac{d}{dz} V_c(z, \omega) = j\omega L(\omega) I_c(z, \omega) \quad (1a)$$

$$-\frac{d}{dz} I_c(z, \omega) = j\omega C(\omega) V_c(z, \omega) \quad (1b)$$

where  $L(\omega)$  and  $C(\omega)$  are the generalized  $N$  by  $N$  inductance and capacitance matrices respectively.

In the quasi-static approximation  $L$  and  $C$  are frequency independent [6]. In [4] it is shown how this quasi-static concept can be extended to cover the full-wave case. As announced in the introduction, we will not go into detail at this point but we will use a relevant example to clarify the concept in relation to previously-published results. It has to be emphasized that (1a) and (1b) are well-suited for CAD applications precisely because they formulate the multiconductor transmission line problem in terms of the familiar telegrapher's equations.

The frequency dependent characteristic impedance matrix  $Z_c(\omega)$  is also very useful for circuit simulation. It follows directly from (1):

$$Z_c(\omega) = [L(\omega)C(\omega)]^{-0.5} L(\omega). \quad (2)$$

This real, symmetric  $N$  by  $N$  matrix is defined in an unambiguous way and can be seen as the input impedance matrix of the infinitely long coupled transmission line structure. The characteristic impedance matrix relates the circuit current waves to the circuit voltage waves traveling in positive longitudinal direction.

### DISCUSSION OF THE CIRCUIT MODEL—EXAMPLE

Now, we analyze a representative asymmetric interconnection structure which was originally described by Fukuoka *et al.* [3]. Fig. 1(a) shows the cross-section of the coupled two-line system. The lines are embedded in an inhomogeneous medium. The structure consists of a perfectly conducting reference conductor, a silicon dioxide layer ( $\text{SiO}_2$ ,  $\epsilon_r = 4$ ) of  $20 \mu\text{m}$  high, and a half-infinite top-layer (air,  $\epsilon_r = 1$ ). The width of both strips is  $10 \mu\text{m}$ . Horizontally, the two strips are separated by  $30 \mu\text{m}$ .

In this structure two fundamental modes can propagate: a c-mode and a  $\pi$ -mode. The longitudinal currents flowing along the conductors are in phase for the c-mode, and in anti-phase for the  $\pi$ -mode. The c-mode corresponds to the even mode in a symmetric structure, while the  $\pi$ -mode corresponds to the odd mode. Note that no even or odd modes can exist in an asymmetrical coupled interconnection structure. In [3], the c- and  $\pi$ -mode seem to be interchanged.